Acta Mech. Sin. (2012) 28(3):825–837
DOI 10.1007/s10409-012-0072-0

RESEARCH PAPER

Parametric study on single shot peening by dimensional analysis method incorporated with finite element method

Xian-Qian Wu · Xi Wang · Yan-Peng Wei · Hong-Wei Song · Chen-Guang Huang

Received: 26 May 2011 / Revised: 10 November 2011 / Accepted: 20 January 2012

Abstract Shot peening is a widely used surface treatment method by generating compressive residual stress near the surface of metallic materials to increase fatigue life and resistance to corrosion fatigue, cracking, etc. Compressive residual stress and dent profile are important factors to evaluate the effectiveness of shot peening process. In this paper, the influence of dimensionless parameters on maximum compressive residual stress and maximum depth of the dent were investigated. Firstly, dimensionless relations of processing parameters that affect the maximum compressive residual stress and the maximum depth of the dent were deduced by dimensional analysis method. Secondly, the influence of each dimensionless parameter on dimensionless variables was investigated by the finite element method. Furthermore, related empirical formulas were given for each dimensionless parameter based on the simulation results. Finally, comparison was made and good agreement was found between the simulation results and the empirical formula, which shows that a useful approach is provided in this paper for analyzing the influence of each individual parameter.

Keywords Shot peening · Maximum compressive residual stress · Maximum depth of the dent · Dimensional analysis method · Finite element method

1 Introduction

Shot peening (SP) is one of the effective surface treatment methods by generating compressive residual stress near the surface of metallic material to increase fatigue life and resistance to corrosion fatigue, cracking, etc [1–5]. It has been widely used in many manufacturing sectors like the aerospace and automobile industries to improve the reliability of structures [6, 7]. The SP process can be seen as a cold working process at room temperature in which small spherical balls are employed to impact a work-piece. With the elastic-plastic interaction between the work-piece and the shots, compressive residual stress is generated near the surface of the work-piece. In recent years, many analytical and numerical models, with which the residual stress, the surface integrity and the influence of parameters can be predicted, have been applied to analyze the SP process to take advantage of advancements in computer technology [5, 6, 8–15]. The effects of some SP parameters have been investigated [2, 16–21], however, little research has focused on systematic analysis of dimensionless parameters in SP process, which is important for clarifying the influence of process conditions. Kelmenz et al. [14] studied the residual stress state after shot peening with dimensional analysis method and finite element method (FEM) simulation, and the effects of four dimensionless input values were investigated. However, the material related dimensionless parameters were not thoroughly studied. In the present paper, a systematic study of dimensionless parameters for single SP process was performed using dimensional analysis method to evaluate the maximum compressive residual stress and the surface integrity. Furthermore, FEM analysis based on LS-DYNA was carried out to simulate the influence of each individual dimensionless parameter. Finally, related empirical formulas were given based on the FEM analysis results, with which the maximum compressive residual stress and the depth of dent could be predicted.

2 Dimensionless parametric analysis

SP is a complex process with multiple variables, such as radius of the shot, impact velocity, material constitutive model

The project was supported by the National Natural Science Foundation of China (10972228, 11002150, and 91016025) and the Basic Research Equipment Project of Chinese Academy of Sciences (YZ200930).

X.-Q. Wu · X. Wang · Y.-P. Wei · H.-W. Song · C.-G. Huang (✉)
Key Laboratory for Hydrodynamics and Ocean Engineering, Institute of Mechanics, Chinese Academy of Sciences, 100190 Beijing, China
e-mail: huangcg@imech.ac.cn

parameters of the shot and work-piece and so on. It is costly and difficult to analyze the influence of each parameter both experimentally and numerically. Dimensional analysis method is an effective method to solve this kind of problems that involves multiple variables. Through appropriate analysis of the relationship between dimensionless variables, the causality of physical phenomena can be highlighted [14, 22–24].

According to the Π theory of dimensional analysis [14, 23, 24], for a problem with n variables $m_1, m_2, \ldots, m_n$, the dependent variable m can be written as

$$m = f(m_1, m_2, \ldots m_k, m_{k+1}, \ldots, m_n), \tag{1}$$

If there are k ($k < n$) independent variables, $m_1, m_2, \ldots, m_k$, then the follow relations can be derived

$$\frac{m}{(m_1^{n_1} m_2^{n_2} \ldots m_k^{n_k})} = f\left(1, 1, \ldots, 1, \frac{m_{k+1}}{(m_1^{p_1} m_2^{p_2} \ldots m_k^{p_k})}, \frac{m_{k+2}}{(m_1^{q_1} m_2^{q_2} \ldots m_k^{q_k})}, \ldots \frac{m_n}{(m_1^{r_1} m_2^{r_2} \ldots m_k^{r_k})}\right). \tag{2}$$

Considering the single SP process, the work-piece can be taken as a semi-infinite medium compared with the shot. As a result, the geometry of the work-piece is excluded in the analysis. A shot with radius R impacts the work-piece at velocity v. The bilinear isotropic hardening model is taken for both the shot and the work-piece, where the effects of strain rate, temperature and viscous are neglected. The friction between the shot and the work-piece is also not considered to simplify the problem. Therefore, parameters of the shot are density ρ_1, Young's modulus E_1, yield stress σ_{Y1}, tangent modulus E_1' and Poisson's ratio ν_1; and parameters of the work-piece are density ρ_2, Young's modulus E_2, yield stress σ_{Y2}, tangent modulus E_2' and Poisson's ratio ν_2, respectively. The related parameters are depicted in Fig. 1.

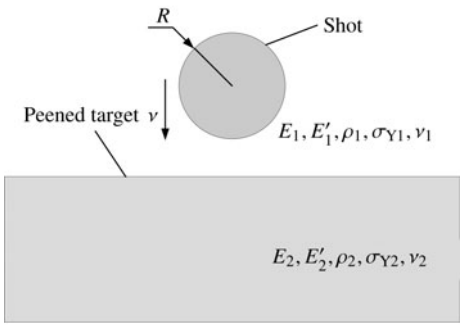

Fig. 1 Related parameters for dimensional analysis

Consequently, the maximum compressive residual stress σ_m and the maximum depth of dent h_m, which are important factors in evaluating the SP effect, are related to these parameters,

$$\sigma_m = f(R, v; \rho_1, E_1, \sigma_{Y1}, E_1', \nu_1; \rho_2, E_2, \sigma_{Y1}, E_2', \nu_2), \tag{3a}$$

$$h_m = f(R, v; \rho_1, E_1, \sigma_{Y1}, E_1', \nu_1; \rho_2, E_2, \sigma_{Y1}, E_2', \nu_2). \tag{3b}$$

Taking the parameters R, ρ_1 and v as independent variables, the following two basic equations can be deduced by dimensional analysis,

$$\frac{\sigma_m}{\rho_1 v^2} = f\left(\frac{\sigma_{Y2}}{\rho_1 v^2}, \frac{\sigma_{Y1}}{\sigma_{Y2}}, \frac{\sigma_{Y2}}{E_2}, \frac{\sqrt{E_2'/\rho_2}}{\sqrt{E_2/\rho_2}}, \frac{\sqrt{E_1/\rho_1}}{\sqrt{E_2/\rho_2}}, \frac{\sqrt{E_1'/\rho_1}}{\sqrt{E_2'/\rho_2}}, \frac{\rho_1}{\rho_2}, \nu_1, \nu_2\right), \tag{4a}$$

$$\frac{h_m}{R} = g\left(\frac{\sigma_{Y2}}{\rho_1 v^2}, \frac{\sigma_{Y1}}{\sigma_{Y2}}, \frac{\sigma_{Y2}}{E_2}, \frac{\sqrt{E_2'/\rho_2}}{\sqrt{E_2/\rho_2}}, \frac{\sqrt{E_1/\rho_1}}{\sqrt{E_2/\rho_2}}, \frac{\sqrt{E_1'/\rho_1}}{\sqrt{E_2'/\rho_2}}, \frac{\rho_1}{\rho_2}, \nu_1, \nu_2\right). \tag{4b}$$

It can be seen that the dimensionless variables $\sigma_m/(\rho_1 v^2)$ and h_m/R are affected by nine dimensionless parameters that are the dimensionless strength of target $\Pi = \sigma_{Y2}/(\rho_1 v^2)$ named yield number which is important for the impact problems, the dimensionless yield stress $\Pi_1 = \sigma_{Y1}/\sigma_{Y2}$, the maximum elastic strain $\Pi_2 = \sigma_{Y2}/E_2$, the dimensionless velocity $\Pi_3 = (E_2'/\rho_2)^{1/2}/(E_2/\rho_2)^{1/2}$ for work-piece, the dimensionless velocity $\Pi_4 = (E_1/\rho_1)^{1/2}/(E_2/\rho_2)^{1/2}$ and $\Pi_5 = (E_1'/\rho_1)^{1/2}/(E_2'/\rho_2)^{1/2}$ of elastic wave and plastic wave, the dimensionless density $\Pi_6 = \rho_1/\rho_2$, the Poisson's ratio $\Pi_7 = \nu_1$ and $\Pi_8 = \nu_2$ for shot and work-piece, respectively.

According to Eq. (4), when the dimensionless parameters are unchanged, the maximum compressive residual stress σ_m depend only on the impact energy density; and the maximum depth of dent h_m is proportional to the radius of the shot, whereas σ_m is independent of it, which is consistent with the conclusions obtained from Refs. [14, 17, 18, 20, 21, 25].

3 FEM validation and virtual experiments

The finite element package LS-DYNA uses an explicit nonlinear structural integration scheme and is suitable for analyzing problems involving impact and contact phenomena, and its application to the simulation of SP process has already been validated by Majzoobi et al. [8] and Hirai et al. [18]. And thus the LS-DYNA code is adopted here to analyze the influence of material characteristics and impact conditions. The shot and work-piece are assumed to have an elasto-plastic behavior described by bilinear isotropic hardening model, as mentioned in Sect. 2.

A 3D symmetric model was developed to ensure the simulation efficiency and enhance the calculation accuracy, as shown in Fig. 2. The shot was meshed with 216 000

SOLID164 elements; and the work-piece was meshed with 512 000 SOLID164 elements, where the impact area is fine meshed to get refined numerical results. The weighted master-slave surface algorithm without considering friction between shot and work-piece was chosen in the LS-DYNA code to simplify the problem.

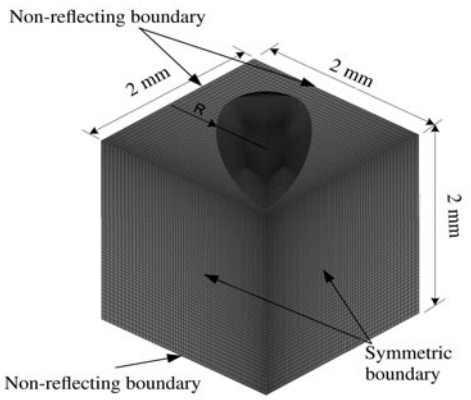

Fig. 2 Numerical model

Firstly, a simulation was conducted to validate the numerical model, in which mild steel is chosen for both the shot and the work-piece. The conditions and material properties used for FEM analysis are presented in Tables 1 and 2. A comparison of the dent profiles between our simulation and experimental results [18] was shown in Fig. 3 for two different shot velocities, where the shot radius is 0.6 mm. The simulation results are found in good agreement with the experiment results, indicating that the proposed numerical model is practicable and reliable in analyzing the influence of parameters.

Table 1 Analysis conditions

Material	Shot velocity $v/(\mathrm{m}\cdot\mathrm{s}^{-1})$	Shot radius R/mm
Shot	20, 50	0.4, 0.5, 0.6

Moreover, to validate the relations derived by dimensional analysis in Sect. 2, parametric studies of different shot radius R and different impact energy density $\rho_1 v^2$ were performed using the numerical model, where the other dimensionless parameters were kept constant. The same material with parameters listed in Table 2 for the elasto-plastic constitutive model was taken for the shot and the work-piece. The simulated results for the two parametric studies are shown in Figs. 4 and 5, which indicates that the maximum compressive residual stress σ_m is not affected by the radius of the shot and depend only on the impact energy density as predicted by Eq. (4a), and the maximum depth of dent h_m is proportional to the radius of the shot when the other dimensionless parameters are kept unchanged, as depicted in Eq. (4b).

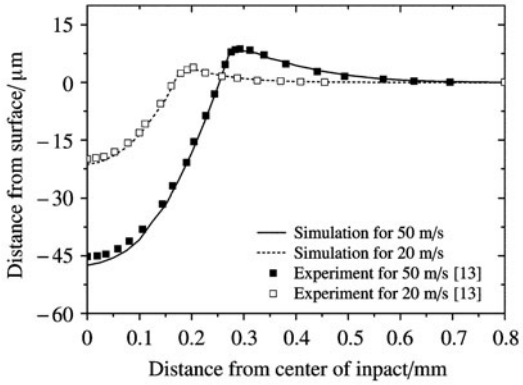

Fig. 3 Dent profile for different shot velocities

Subsequently, the finite element method was used to analyze the influence of each dimensionless parameter appearing in Eq. (4) using numerical simulation. The simulation conditions assigned for influence analysis of the nine dimensionless parameters are shown in Table 3. The same material constitutive model was taken whereas the material parameters under study vary for each case of parameter analysis. Here, a decoupled fitting method is taken to obtain the influence formulas for each dimensionless parameter. While one dimensionless parameter Π_α is studied, the other un-fitted dimensionless parameters are kept unchanged. As a result, the influence of Π_α could be fitted by a formula $f_\alpha(\Pi_\alpha)$. With this method, the influence of an individual dimensionless parameter could be fitted by a corresponding formula, and Eq. (4) could be finally re-written as

$$\begin{aligned}\frac{\sigma_\mathrm{m}}{\rho_1 v^2} &= f_0\left(\frac{\sigma_{\mathrm{Y}2}}{\rho_1 v^2}\right) f_1\left(\frac{\sigma_{\mathrm{Y}1}}{\sigma_{\mathrm{Y}2}}\right) f_2\left(\frac{\sigma_{\mathrm{Y}2}}{E_2}\right) f_3\left(\frac{\sqrt{E_2'/\rho_2}}{\sqrt{E_2/\rho_2}}\right)\\ &\quad\times f_4\left(\frac{\sqrt{E_1/\rho_1}}{\sqrt{E_2/\rho_2}}\right) f_5\left(\frac{\sqrt{E_1'/\rho_1}}{\sqrt{E_2/\rho_2}}\right) f_6\left(\frac{\rho_1}{\rho_2}\right)\\ &\quad\times f_7(\nu_1)\, f_8(\nu_2)\\ \frac{h_\mathrm{m}}{R} &= g_0\left(\frac{\sigma_{\mathrm{Y}2}}{\rho_1 v^2}\right) g_1\left(\frac{\sigma_{\mathrm{Y}1}}{\sigma_{\mathrm{Y}2}}\right) g_2\left(\frac{\sigma_{\mathrm{Y}2}}{E_2}\right) g_3\left(\frac{\sqrt{E_2'/\rho_2}}{\sqrt{E_2/\rho_2}}\right)\\ &\quad\times g_4\left(\frac{\sqrt{E_1/\rho_1}}{\sqrt{E_2/\rho_2}}\right) g_5\left(\frac{\sqrt{E_1'/\rho_1}}{\sqrt{E_2/\rho_2}}\right) g_6\left(\frac{\rho_1}{\rho_2}\right)\\ &\quad\times g_7(\nu_1)\, g_8(\nu_2)\end{aligned}$$

Table 2 Material properties used for FEM analysis [18]

Material	Density $/(\mathrm{g}\cdot\mathrm{cm}^{-3})$	Young's modulus/GPa	Poisson's ratio	Yield /MPa	Tangent modulus GPa stress/MPa
Shot	7.8	210	0.28	500	2.0
Work-piece	7.8	210	0.28	300	1.2

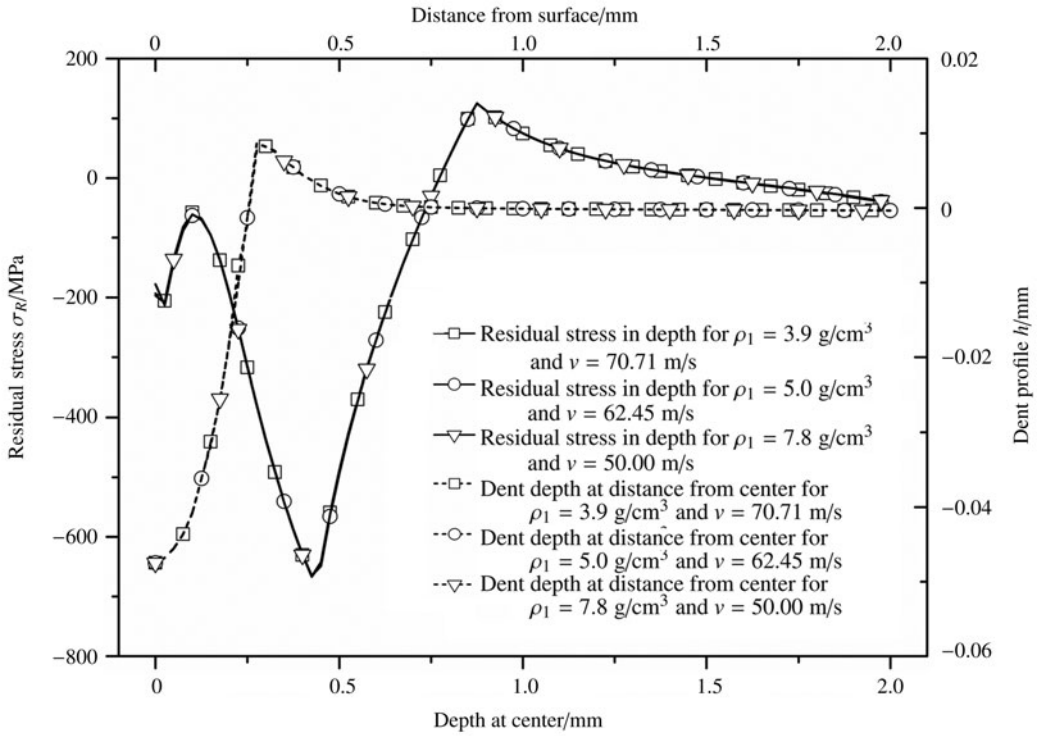

Fig. 4 Residual stress distributions in depth and dent profiles for the same impact energy density

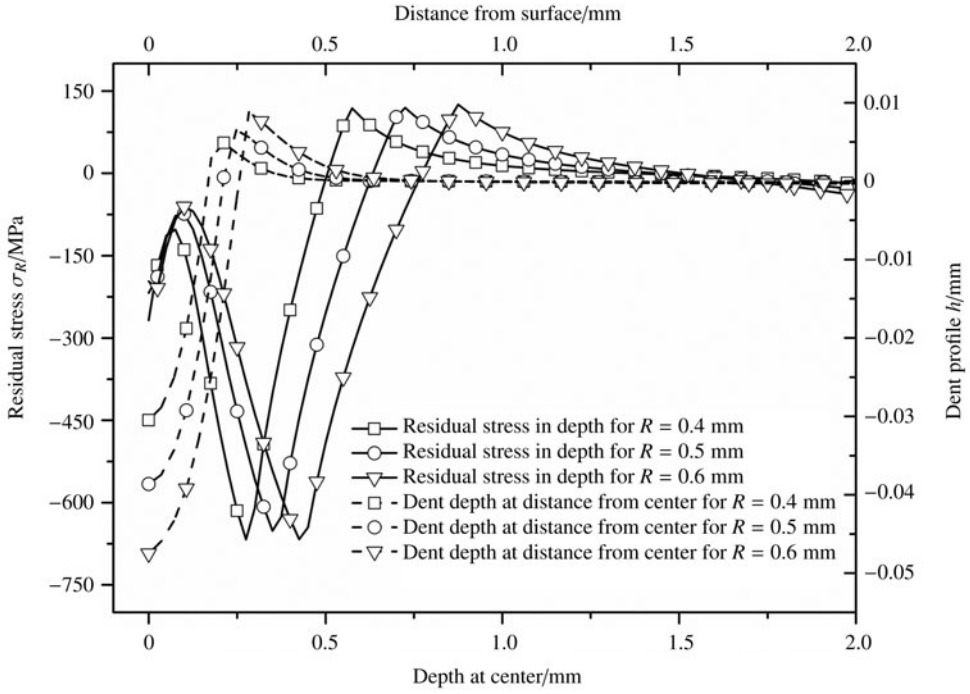

Fig. 5 Residual stress distributions in depth and dent profiles for different shot radii

Table 3 Assigned conditions for dimensionless parameters studies

Dimensionless parameters	$\sigma_{Y2}/(\rho_1 v^2)$	σ_{Y1}/σ_{Y2}	σ_{Y2}/E_2	$(E_2'/\rho_2)^{1/2}/(E_2/\rho_2)^{1/2}$	$(E_1/\rho_1)^{1/2}/(E_2/\rho_2)^{1/2}$	$(E_1'/\rho_1)^{1/2}/(E_2'/\rho_2)^{1/2}$	ρ_1/ρ_2	ν_1	ν_2
Designed parameters	v	σ_{Y1}	σ_{Y2}, and σ_{Y1}/σ_{Y2} constant	E_2, and E_1/E_2 constant	E_1	E_1'	ρ_1/ρ_2	ν_1	ν_2

4 Results and discussions

The influence of yield number $\sigma_{Y2}/(\rho_1 v^2)$ on the dimensionless stress $\sigma_m/(\rho_1 v^2)$ and the dimensionless depth h_m/R was shown in Fig. 6. The empirical relationships of $\sigma_{Y2}/(\rho_1 v^2)$ to $\sigma_m/(\rho_1 v^2)$ and h_m/R could be derived from the formula fitting of the simulated data as

$$f_0\left(\frac{\sigma_{Y2}}{\rho_1 v^2}\right) = 1.506 - \frac{2.345\sigma_{Y2}}{\rho_1 v^2}, \tag{5a}$$

$$g_0\left(\frac{\sigma_{Y2}}{\rho_1 v^2}\right) = 0.241\,5\left(\frac{\sigma_{Y2}}{\rho_1 v^2}\right)^{-0.410\,9}. \tag{5b}$$

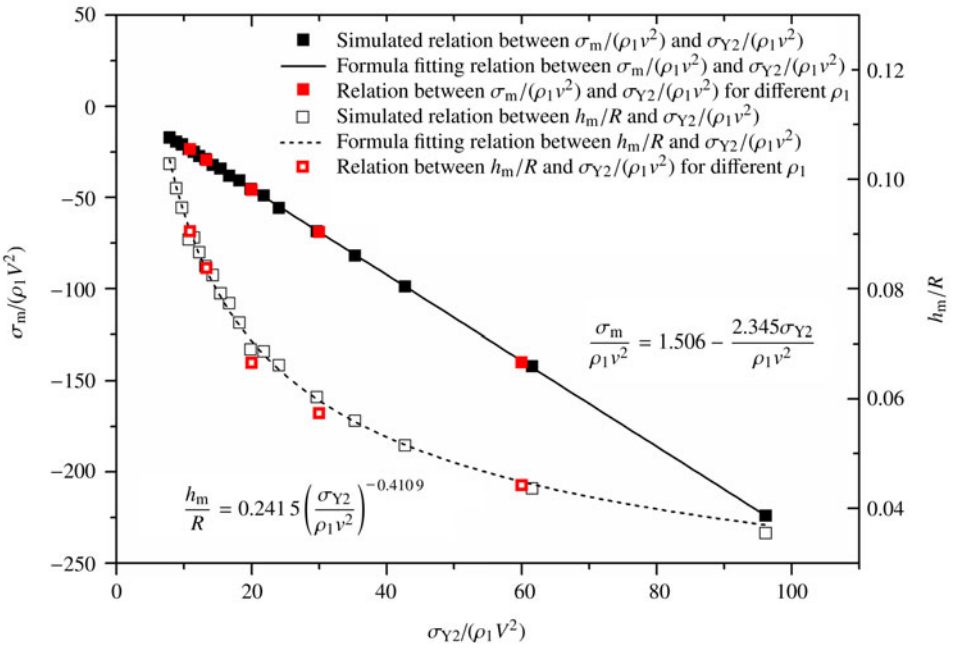

Fig. 6 The influence of the yield number $\sigma_{Y2}/(\rho_1 v^2)$

Figure 6 shows that the yield number is an important number for the effectiveness of SP. The dimensionless stress and depth increase greatly as the yield number decreases.

To validate the decoupling fitting method, the influences of yield number $\sigma_{Y2}/(\rho_1 v^2)$ on the dimensionless stress $\sigma_m/(\rho_1 v^2)$ and the dimensionless depth h_m/R are simulated for different shot densities ρ_1, where the dimensionless density ρ_1/ρ_2 is kept unchanged to eliminate the influence of other dimensional parameters. As depicted in Fig. 6, the simulated results agree well with the formula fitting results, which demonstrate the validity of the decoupling fitting method. A further validation simulation is performed, where the variables ρ_1, E_1, σ_{Y1}, E_1', ρ_2, E_2, σ_{Y2}, E_2', are chosen as the values considered originally multiplied with a coefficient γ to make sure the other dimensionless parameters remain unchanged. The simulated dimensionless peening effects, $\sigma_m/(\rho_1 v^2)$ and h_m/R, are list in Table 4. The simulated results are almost unchanged and consistent with the dimensional analysis and Eq. (14). Therefore, the influences of the other dimensionless parameters could also be fitted by formulas using this method.

Table 4 Simulated dimensionless peening effects for different γ

γ	$\sigma_m/(\rho_1 v^2)$	h_m/R
0.5	−34.14	7.919×10^{-2}
1.0	−34.14	7.919×10^{-2}
1.5	−34.12	7.918×10^{-2}

The influence of the dimensionless yield stress σ_{Y1}/σ_{Y2} on the dimensionless variable $\sigma_m/[(\rho_1 v^2) f(\Pi)]$ and $h_m/[Rg(\Pi)]$ was shown in Fig. 7, from which the influence relations can be obtained as

$$f_1\left(\frac{\sigma_{Y1}}{\sigma_{Y2}}\right) = 1.047 - 1.124\exp\left(-\frac{\sigma_{Y1}}{0.547\,7\sigma_{Y2}}\right), \tag{6a}$$

$$g_1\left(\frac{s_{Y1}}{s_{Y2}}\right) = 1.198 - \frac{1.198}{1 + \exp\left(\dfrac{\sigma_{Y1}/\sigma_{Y2} - 1.217}{0.295\,2}\right)}, \tag{6b}$$

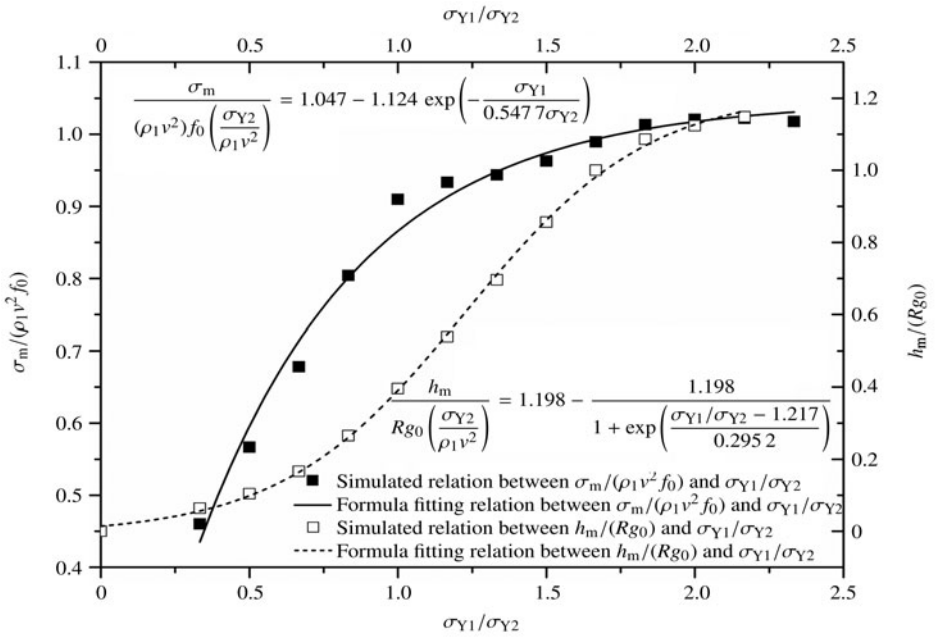

Fig. 7 The influence of the dimensionless yield stress σ_{Y1}/σ_{Y2}

The influence of the maximum elastic strain σ_{Y2}/E_2 on the dimensionless variable $\sigma_m/[(\rho_1 v^2) f(\Pi) f_1(\Pi_1)]$ and $h_m/[Rg(\Pi) g_1(\Pi_1)]$ was shown in Fig. 8, which shows that the effect of maximum elastic strain of the work-piece is insignificant. The corresponding relations could be obtained as

$$f_2\left(\frac{\sigma_{Y2}}{E_2}\right) = 1.023 - 5.090 \times 10^{-3} \exp\left(\frac{10^4 \sigma_{Y2}}{9.262 E_2}\right), \tag{7a}$$

$$g_2\left(\frac{\sigma_{Y2}}{E_2}\right) = 1.081 - 1.106 \exp\left(-\frac{10^4 \sigma_{Y2}}{5.300 E_2}\right). \tag{7b}$$

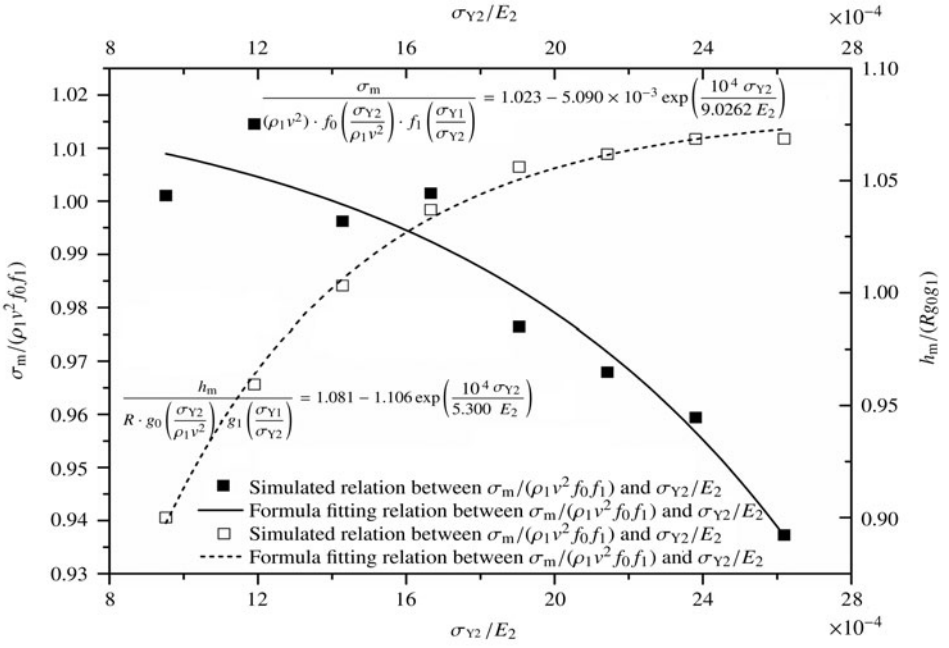

Fig. 8 The influence of the maximum elastic strain σ_{Y2}/E_2

The influence of the dimensionless velocity ratio of plastic to elastic wave velocities $(E_2'/\rho_2)^{1/2}/(E_2/\rho_2)^{1/2}$ on the dimensionless variable $\sigma_m/[(\rho_1 v^2)f(\Pi)f_1(\Pi_1)f_2(\Pi_2)]$ and $h_m/[Rg(\Pi)g_1(\Pi_1)g_2(\Pi_2)]$ was shown in Fig. 9. The influence relations are obtained as

$$f_3\left(\frac{\sqrt{E_2'/\rho_2}}{\sqrt{E_2/\rho_2}}\right) = 0.987\,1 + 5.463\,5\exp\left(-\frac{100\sqrt{E_2'/\rho_2}}{1.164\sqrt{E_2/\rho_2}}\right), \tag{8a}$$

$$g_3\left(\frac{\sqrt{E_2'/\rho_2}}{\sqrt{E_2/\rho_2}}\right) = 0.913\,0 + 18.53\exp\left(-\frac{100\sqrt{E_2'/\rho_2}}{1.395\times\sqrt{E_2/\rho_2}}\right). \tag{8b}$$

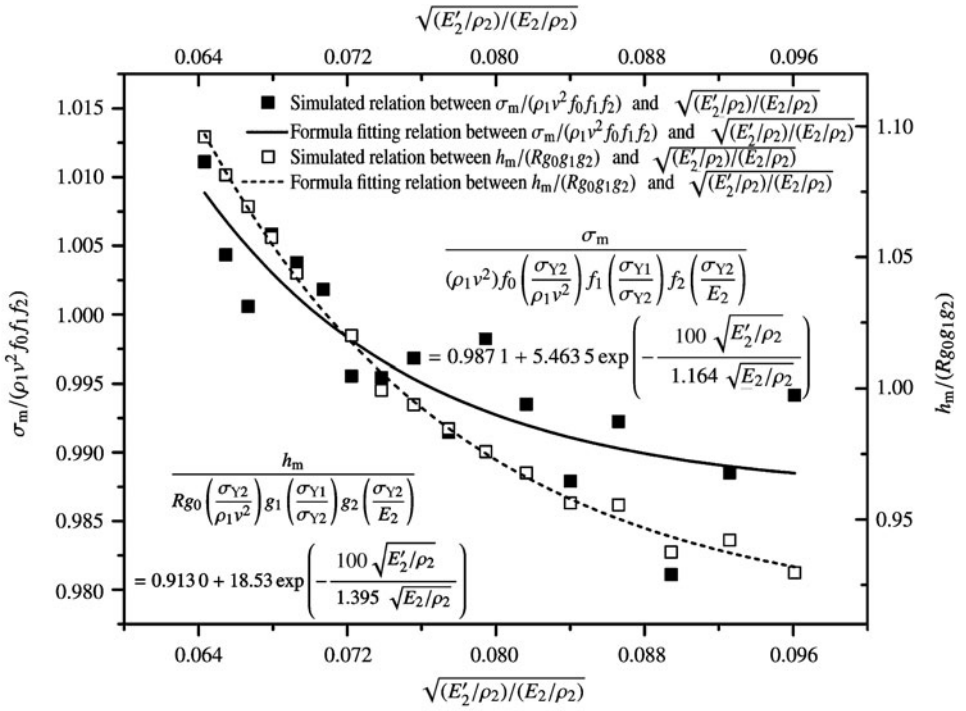

Fig. 9 The influence of the dimensionless ratio of plastic to elastic wave velocities

The influence of dimensionless elastic wave velocity $(E_1/\rho_1)^{1/2}/(E_2/\rho_2)^{1/2}$ on the dimensionless variable $\sigma_m/[(\rho_1 v^2)f(\Pi)f_1(\Pi_1)f_2(\Pi_2)f_3(\Pi_3)]$ and $h_m/[Rg(\Pi)g_1(\Pi_1)g_2(\Pi_2)g_3(\Pi_3)]$ was shown in Fig. 10. The effect of the dimensionless elastic wave velocity could be neglected for dimensionless stress. Therefore, the influence relations can be obtained as follows,

$$f_4\left(\frac{\sqrt{E_1/\rho_1}}{\sqrt{E_2/\rho_2}}\right) = 1, \tag{9a}$$

$$g_4\left(\frac{\sqrt{E_1/\rho_1}}{\sqrt{E_2/\rho_2}}\right) = 1.103 - 0.586\,2\exp\left(-\frac{\sqrt{E_1/\rho_1}}{0.586\,0\sqrt{E_2/\rho_2}}\right). \tag{9b}$$

The influence of dimensionless plastic wave velocity $(E_1'/\rho_1)^{1/2}/(E_2'/\rho_2)^{1/2}$ on the dimensionless variable $\sigma_m/[(\rho_1 v^2)f(\Pi)f_1(\Pi_1)f_2(\Pi_2)f_3(\Pi_3)f_4(\Pi_4)]$ and $h_m/[Rg(\Pi)g_1(\Pi_1)g_2(\Pi_2)g_3(\Pi_3)g_4(\Pi_4)]$ was shown in Fig. 11. Similarly, the influence relations can be obtained as

$$f_5\left(\frac{\sqrt{E_1'/\rho_1}}{\sqrt{E_2'/\rho_2}}\right) = 1.024 - \frac{0.019\,31\sqrt{E_1'/\rho_1}}{\sqrt{E_2'/\rho_2}}, \tag{10a}$$

$$g_5\left(\frac{\sqrt{E_1'/\rho_1}}{\sqrt{E_2'/\rho_2}}\right) = 0.884\,2 - \frac{0.091\,48\sqrt{E_1'/\rho_1}}{\sqrt{E_2'/\rho_2}}. \tag{10b}$$

The influence of dimensionless density ρ_1/ρ_2 on the dimensionless variable $\sigma_m/[(\rho_1 v^2)f(\Pi)f_1(\Pi_1)f_2(\Pi_2)f_3(\Pi_3)f_4(\Pi_4)f_5(\Pi_5)]$ and $h_m/[Rg(\Pi)g_1(\Pi_1)g_2(\Pi_2)g_3(\Pi_3)g_4(\Pi_4)g_5(\Pi_5)]$ was shown in Fig. 12. Concerning the influence of the dimensionless density ρ_1/ρ_2, the following relations can be obtained as

$$f_6\left(\frac{\rho_1}{\rho_2}\right) = 1.100 - 0.150\,1\exp\left(-\frac{\rho_1}{2.368\rho_2}\right), \tag{11a}$$

$$g_6\left(\frac{\rho_1}{\rho_2}\right) = 1.106 - 0.392\,5\exp\left(-\frac{\rho_1}{0.781\,7\rho_2}\right). \tag{11b}$$

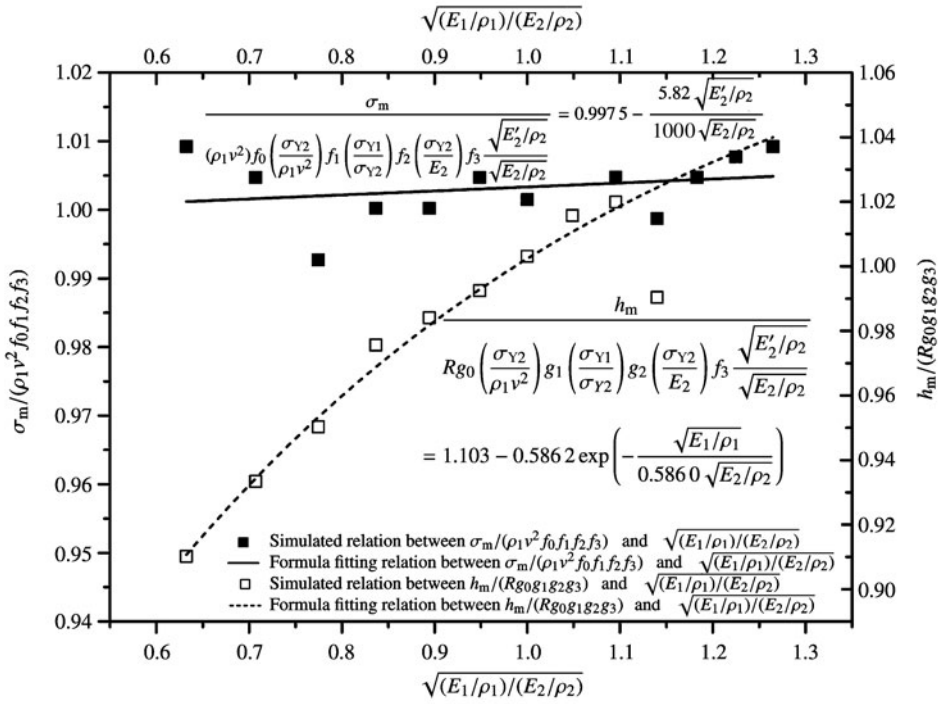

Fig. 10 The influence of dimensionless elastic wave velocity $(E_1/\rho_1)^{1/2}/(E_2/\rho_2)^{1/2}$

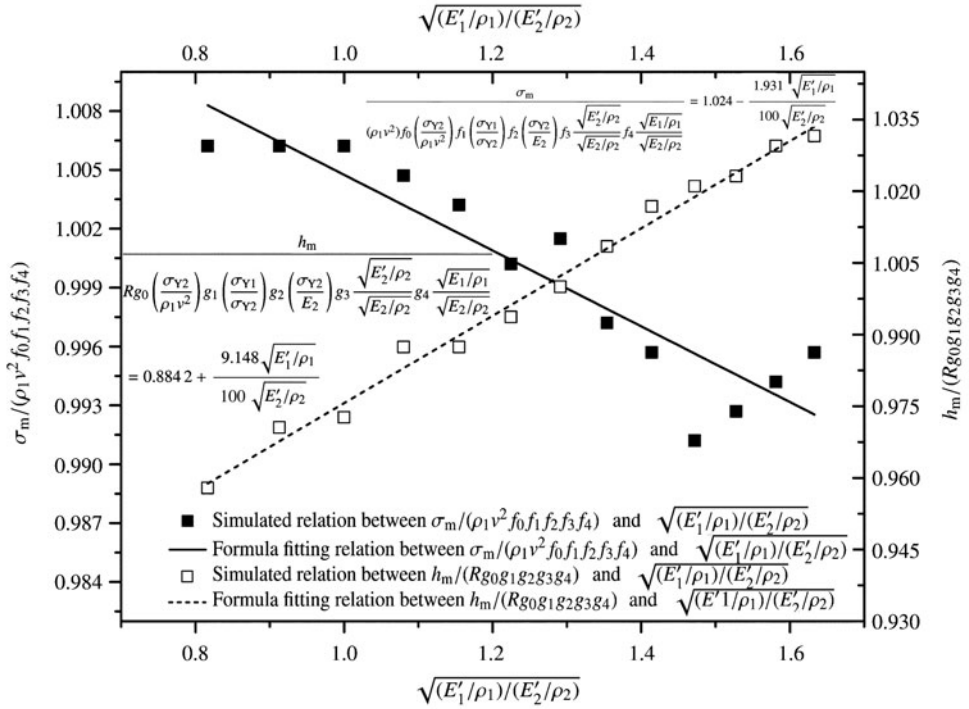

Fig. 11 The influence of dimensionless plastic wave velocity $(E_1'/\rho_1)^{1/2}/(E_2'/\rho_2)^{1/2}$

Additionally, the influences of Poisson's ratio ν_1 and ν_2 were investigated as shown in Figs. 13 and 14. By the same method, the following relations can be derived,

$$f_7(\nu_1) = 1.000, \tag{12a}$$

$$g_7(\nu_1) = 1.000, \tag{12b}$$

$$f_8(\nu_2) = 1.000, \tag{13a}$$

$$g_8(\nu_2) = 1.000. \tag{13b}$$

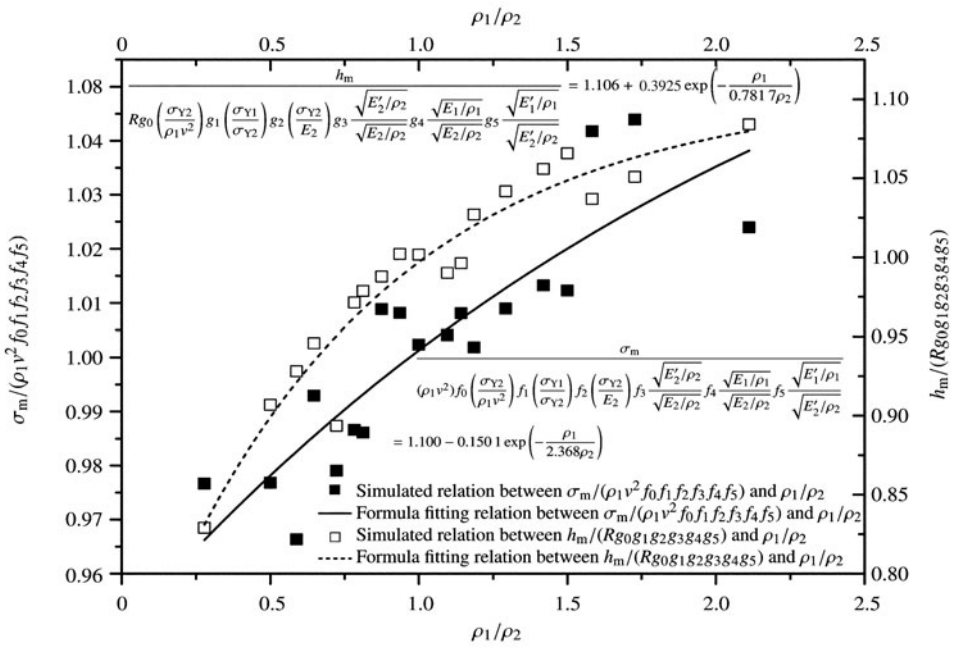

Fig. 12 The influence of dimensionless density ρ_1/ρ_2

It also indicates that the effects of Poisson's ratio are insignificant in the range from 0.20 to 0.36, and therefore it can be neglected in the present analysis.

In summary, the influences of the parameters on the maximum compressive residual stress and the maximum depth of the dent can be obtained by multiplying these influence relations corresponding to each dimensionless parameters, where the influence of Poisson's ratio was not taken into account.

$$\frac{\sigma_m}{\rho_1 v^2} = f_0\left(\frac{\sigma_{Y2}}{\rho_1 v^2}\right) f_1\left(\frac{\sigma_{Y1}}{\sigma_{Y2}}\right) f_2\left(\frac{\sigma_{Y2}}{E_2}\right) f_3\left(\frac{\sqrt{E_2'/\rho_2}}{\sqrt{E_2/\rho_2}}\right) \times f_4\left(\frac{\sqrt{E_1/\rho_1}}{\sqrt{E_2/\rho_2}}\right) f_5\left(\frac{\sqrt{E_1'/\rho_1}}{\sqrt{E_2'/\rho_2}}\right) f_6\left(\frac{\rho_1}{\rho_2}\right), \tag{14a}$$

$$\frac{h_m}{R} = g_0\left(\frac{\sigma_{Y2}}{\rho_1 v^2}\right) g_1\left(\frac{\sigma_{Y1}}{\sigma_{Y2}}\right) g_2\left(\frac{\sigma_{Y2}}{E_2}\right) g_3\left(\frac{\sqrt{E_2'/\rho_2}}{\sqrt{E_2/\rho_2}}\right) \times g_4\left(\frac{\sqrt{E_1/\rho_1}}{\sqrt{E_2/\rho_2}}\right) g_5\left(\frac{\sqrt{E_1'/\rho_1}}{\sqrt{E_2'/\rho_2}}\right) g_6\left(\frac{\rho_1}{\rho_2}\right). \tag{14b}$$

Here

$$f_0\left(\frac{\sigma_{Y2}}{\rho_1 v^2}\right) = 1.506 - \frac{2.345\sigma_{Y2}}{\rho_1 v^2},$$

$$f_1\left(\frac{\sigma_{Y1}}{\sigma_{Y2}}\right) = 1.047 - 1.124 \times \exp\left(-\frac{\sigma_{Y1}}{0.547\,7\sigma_{Y2}}\right),$$

$$f_2\left(\frac{\sigma_{Y2}}{E_2}\right) = 1.023 - 5.090 \times 10^{-3}\exp\left(\frac{10^4\sigma_{Y2}}{9.262E_2}\right),$$

$$f_3\left(\frac{\sqrt{E_2'/\rho_2}}{\sqrt{E_2/\rho_2}}\right) = 0.987\,1 + 5.464\exp\left(-\frac{100\sqrt{E_2'/\rho_2}}{1.164\sqrt{E_2/\rho_2}}\right),$$

$$f_4\left(\frac{\sqrt{E_1/\rho_1}}{\sqrt{E_2/\rho_2}}\right) = 1,$$

$$f_5\left(\frac{\sqrt{E_1'/\rho_1}}{\sqrt{E_2'/\rho_2}}\right) = 1.024 - 0.01931\frac{\sqrt{E_1'/\rho_1}}{\sqrt{E_2'/\rho_2}},$$

$$f_6\left(\frac{\rho_1}{\rho_2}\right) = 1.1 - 0.150\,1\exp\left(-\frac{\rho_1}{2.368\rho_2}\right)$$

and

$$g_0\left(\frac{\sigma_{Y2}}{\rho_1 v^2}\right) = 0.241\,5\left(\frac{\sigma_{Y2}}{\rho_1 v^2}\right)^{-0.410\,9},$$

$$g_1\left(\frac{s_{Y1}}{s_{Y2}}\right) = 1.198 - \frac{1.198}{1+\exp\left(\frac{\sigma_{Y1}/\sigma_{Y2} - 1.217}{0.295\,2}\right)},$$

$$g_2\left(\frac{\sigma_{Y2}}{E_2}\right) = 1.081 - 1.106\exp\left(-\frac{10^4\sigma_{Y2}}{5.3E_2}\right),$$

$$g_3\left(\frac{\sqrt{E_2'/\rho_2}}{\sqrt{E_2/\rho_2}}\right) = 0.913 + 18.53\exp\left(-\frac{100\sqrt{E_2'/\rho_2}}{1.395\sqrt{E_2/\rho_2}}\right),$$

$$g_4\left(\frac{\sqrt{E_1/\rho_1}}{\sqrt{E_2/\rho_2}}\right) = 1.103 - 0.586\,2\exp\left(-\frac{\sqrt{E_1/\rho_1}}{0.586\sqrt{E_2/\rho_2}}\right),$$

$$g_5\left(\frac{\sqrt{E_1'/\rho_1}}{\sqrt{E_2'/\rho_2}}\right) = 0.884\,2 + \frac{9.148\sqrt{E_1'/\rho_1}}{100\sqrt{E_2'/\rho_2}},$$

$$g_6\left(\frac{\rho_1}{\rho_2}\right) = 1.106 - 0.392\,5\exp\left(-\frac{\rho_1}{0.781\,7\rho_2}\right).$$

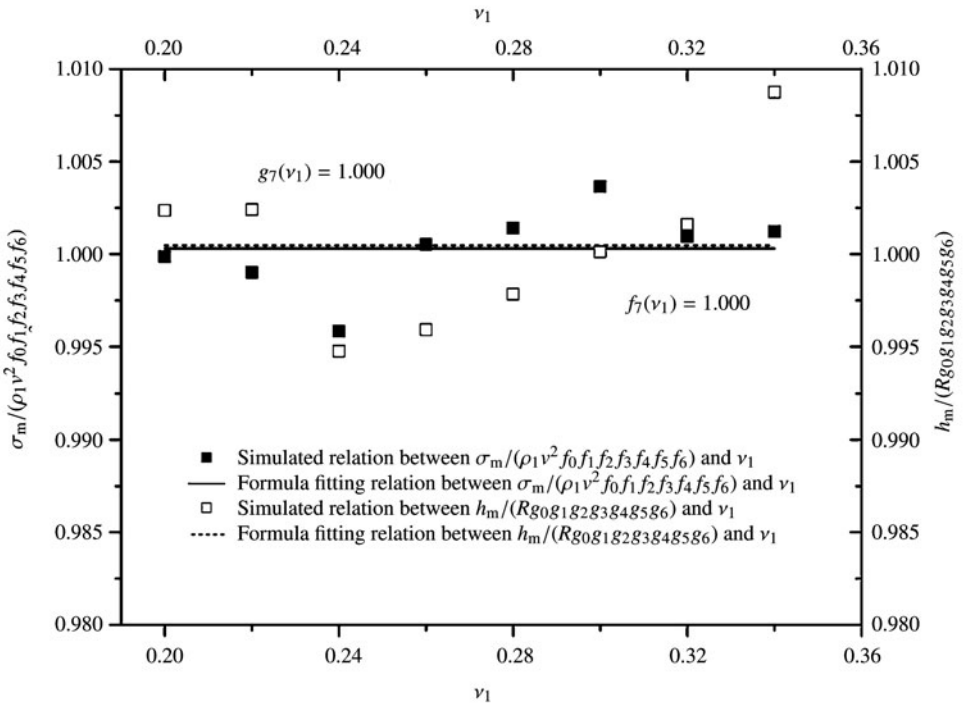

Fig. 13 The influences of Poisson's ratio ν_1

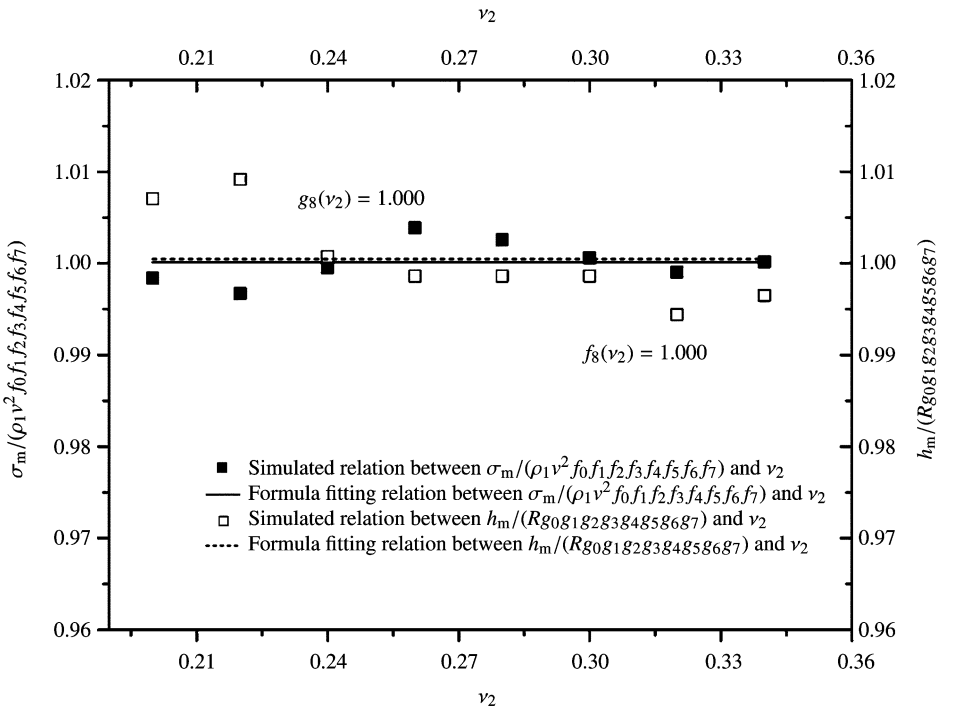

Fig. 14 The influences of Poisson's ratio ν_2

In the present study, the influences of the dimensionless parameters are deduced by the decoupled fitting method. In fact, the influences of these dimensionless parameters are not independent of each other. For instance, if the variable σ_{Y2} is changed, the influences of dimensionless parameters $\sigma_{Y2}/(\rho_1 v^2)$, σ_{Y1}/σ_{Y2}, and σ_{Y2}/E_2 are coupled with each other. However, the decoupling fitting method provides a useful method to obtain the influence corresponding to each dimensionless parameter. After the influence of $\sigma_{Y2}/(\rho_1 v^2)$ is obtained, its coupled influence on σ_{Y1}/σ_{Y2} could be cal-

culated, and then the influence of σ_{Y1}/σ_{Y2} could be fitted. The dependence of the peening effect on other dimensionless parameters can be derived similarly.

In view of the formulas f_1 to f_6 and g_1 to g_6, the values of f_3 to f_6 and g_3 to g_6 change slightly in the parameter range we studied. When the effects of these formulas are neglected, the following relations could be deduced as a rough estimation,

$$\frac{\partial\sigma_m}{\partial\rho_1} > 0, \quad \frac{\partial\sigma_m}{\partial v} > 0, \quad \frac{\partial\sigma_m}{\partial R} = 0, \quad \frac{\partial\sigma_m}{\partial\sigma_{Y1}} > 0,$$
$$\frac{\partial\sigma_m}{\partial\sigma_{Y2}} < 0, \quad \frac{\partial h_m}{\partial\rho_1} > 0, \quad \frac{\partial h_m}{\partial v} > 0, \quad \frac{\partial h_m}{\partial R} > 0,$$
$$\frac{\partial h_m}{\partial\sigma_{Y1}} > 0, \quad \frac{\partial h_m}{\partial\sigma_{Y2}} < 0.$$

Therefore, to obtain a good peening effect with higher compressive residual stress and smaller depth of dent, the size of the shot should be as small as possible, which is consistent with the dimensional analyses result. In addition, increasing impact energy density and yield stress of the shot would increase σ_m. Nevertheless, it also increases the depth of dent profile and leads to a rough appearance of the workpiece surface, which could be improved by multiple shots process.

If the material-related parameters are kept unchanged, the material related dimensionless parameters will be constant. As a result, Eq. (14) can be written as

$$\frac{\sigma_m}{\rho_1 v^2} = k_{11} f_0\left(\frac{\sigma_{Y2}}{\rho_1 v^2}\right), \tag{15a}$$

$$\frac{h_m}{R} = k_{12} g_0\left(\frac{\sigma_{Y2}}{\rho_1 v^2}\right). \tag{15b}$$

Hirai et al. [18] obtained the relation of the depth of dent with the shot diameter and the shot velocity as

$$h_m = k_1 D v^{9/10} \tag{16}$$

Although the value of power exponent in the present Eq. (15b) and that of Hirai et al.'s relation are a little different, both relations are similar to each other. The comparison of the impact velocity's influence on the maximum depth of dent between the empirical Eqs. (15b) and (16) was shown in Fig. 15, from which it could be seen that the present Eqs. (15b) and (16) both fitted the simulation results very well.

Furthermore, the comparison of the results from simulation and empirical formula with different parameters was listed in Table 5, where σ_{me}, h_{me} were results calculated with empirical Eq. (14) and σ_{ms}, h_{ms} were simulated results by LS-DYNA. The results obtained by empirical formulas are in good agreement with the simulated results. The maximum differences are less than 4.9% for the maximum compressive residual stress and 7.1% for the maximum depth of the dent. Finally, the empirical formulas were validated with experimental data [18] as shown in Fig. 16. The analytical result of empirical formulas is also in good agreement with the experiment results, which shows the applicability of the empirical formulas to predict the maximum compressive residual stress and maximum depth of the dent for single SP process. However, the influence of the friction between the shot and the work-piece is neglected in the present research. It will be studied in the future. In addition, other variables, such as the depth of the compressive residual stress, the position of the maximum compressive residual stress and the other dimension of the dent, can also be obtained in the same way. Although this analysis method is based on single SP, similar empirical formulas can be deduced as well for multiple shot peening with this method by introducing relevant dimensionless parameters.

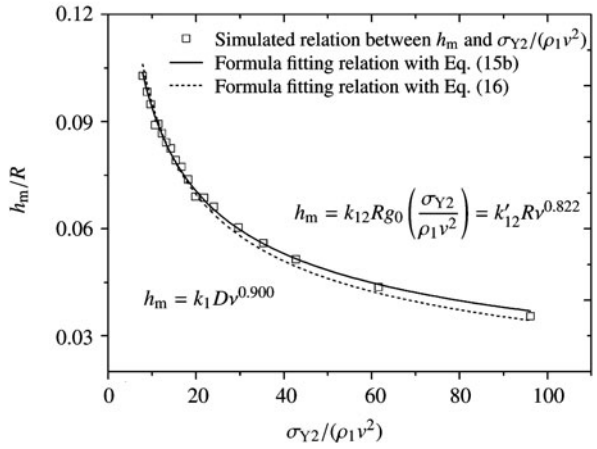

Fig. 15 The comparison of the impact velocity's influence on the maximum depth of dent between the empirical Eqs. (15b) and (16)

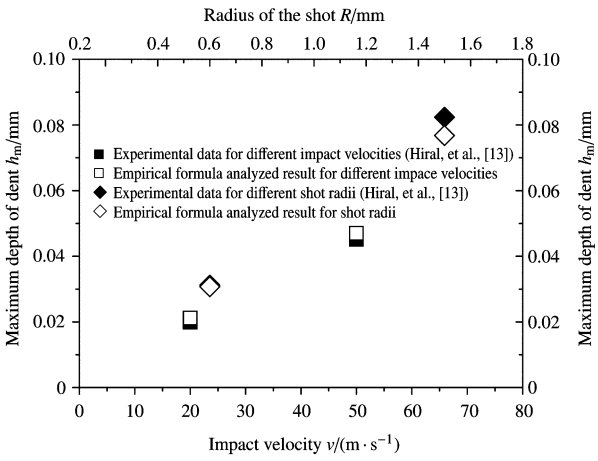

Fig. 16 The comparison of empirical formulas and experimental data

Table 5 Comparison of the simulation results and the empirical formula for different parameters

R/mm	v	$\rho_1/(\mathrm{g\cdot cm^{-3}})$	E_1/GPa	E_1'/GPa	σ_{Y1}/MPa	ν_1	$\rho_2/(\mathrm{g\cdot cm^3})$	E_2/GPa	E_2'/GPa	σ_{Y2}/MPa	ν_1	σ_{me}/GPa	σ_{ms}/GPa	h_{me}/mm	h_{ms}/mm
0.6	50	5.2	190	1.6	600	0.35	6.8	180	1.5	450	0.26	–0.913	–0. 905	0.024	0.025
0.6	40	6.9	230	2.1	450	0.28	5.4	175	1.1	280	0.28	–0. 632	–0. 642	0.038	0.039
0.6	60	7.2	210	1.9	500	0.29	6.5	200	1.3	320	0.29	–0. 695	–0. 706	0.047	0.047
0.6	37	6.5	200	1.8	760	0.33	7.5	195	1.2	550	0.3	– 1.105	–1.161	0.021	0.021
0.6	45	4.8	200	2.4	550	0.31	7.9	205	1.9	500	0.27	–0. 957	–0. 932	0.014	0.014
0.6	69	8.8	210	2.0	650	0.26	7.5	220	1.4	290	0.29	–0. 639	–0. 635	0.071	0.076
0.6	55	6.5	220	2.0	500	0.28	6.2	210	1.2	340	0.31	–0. 739	–0. 742	0.039	0.039
0.6	75	7.5	220	2.1	550	0.28	8.4	200	1.4	420	0.28	–0. 836	–0. 820	0.040	0.038
0.6	82	5.5	200	1.8	650	0.34	4.9	190	1.0	270	0.28	–0. 598	–0. 603	0.076	0.079

5 Conclusions

In the present paper, the influence of dimensionless parameters for single SP process were studied using dimensional analysis method and FEM simulation to evaluate the compressive residual stress and the peened surface quality. The main conclusions are drawn as follows,

(1) The dimensionless parameters affecting the maximum compressive residual stress and the maximum depth of the dent were obtained by dimensional analysis method. Accordingly, a possible systematic analysis method is provided for single SP process.

(2) The influences of each dimensionless parameter were investigated by FEM simulation. Furthermore, empirical formulas for these dimensionless parameters were obtained based on FEM simulation results and validated by experiment results, which shows that an effective method is provided here to analyze the influences of each individual parameters. More experiments will be carried out to validate this analysis approach in the future.

(3) Although the present research focuses on the single SP process, it provides a potential method to analyze the influences of parameters in multiple SP process in the same way by introducing relevant dimensionless parameters.

References

1 Zimmermann, M., Klemenz, M., Schulze, V.: Literature review on shot peening simulation. International Journal of Computational Materials Science and Surface Engineering **3**, 289–310 (2010)

2 Miao, H. Y., Demers, D., Larose, S., et al.: Experimental study of shot peening and stress peen forming. Journal of Materials Processing Technology **210**, 2089–2102 (2010)

3 Lindemann, J., Buque, C., Appel, F.: Effect of shot peening on fatigue performance of a lamellar titanium aluminide alloy. Acta Materialia **54**, 1155–1164 (2006)

4 Tosha, K., Ueno, Y., Iida, K.: Effect of shot peening on fatigue strength of phosphor bronze C5191. Shotto Piningu Gijutsu **11**, 101–106 (1999)

5 Klemenz, M., Schulze, V., Rohr, I., et al.: Application of the FEM for the prediction of the surface layer characteristics after shot peening. Journal of Materials Processing Technology **209**, 4093–4102 (2009)

6 Frija, M., Hassine, T., Fathallah, R., et al.: Finite element modelling of shot peening process: Prediction of the compressive residual stresses, the plastic deformations and the surface integrity. Materials Science and Engineering: A **426**, 173–180 (2006)

7 Gao, Y. K.: Improvement of fatigue property in 7050-T7451 aluminum alloy by laser peening and shot peening. Materials Science and Engineering: A **10–11**, 3823–3828 (2011)

8 Majzoobi, G. H., Azizi, R., Alavi Nia, A.: A three-dimensional simulation of shot peening process using multiple shot impacts. Journal of Materials Processing Technology **164–165**, 1226–1234 (2005)

9 Meguid, S. A., Shagal, G., Stranart, J. C., et al.: Three-dimensional dynamic finite element analysis of shot-peening induced residual stresses. Finite Elements in Analysis and Design **31**, 179–191 (1999)

10 Meo, M., Vignjevic, R.: Finite element analysis of residual stress induced by shot peening process. Advances in Engineering Software **34**, 569–575 (2003)

11 Shen, S., Atluri, S.: An analytical model for shot-peening induced residual stresses. Computers, Materials and Continua **4**, 75–85 (2006)

12 Li, J. K., Mei, Y., Duo, W., et al.: Mechanical approach to the residual stress field induced by shot peening. Materials Science and Engineering: A **147**, 167–173 (1991)

13 Hirai, N., Tosha, K.: Finite element analyses of shot peening traces with respect to work-hardening factor. Shotto Piningu Gijutsu **17**, 123–129 (2005)

14 Klemenz, M., Zimmermann, M., Schulze, V., et al.: Numerical prediction of the residual stress state after shot peening. High Performance Computing in Science and Engineering **5**, 437–448 (2007)

15 Zimmermann, M., Klemenz, M., Schulze, V., et al.: Numerical studies on the influence of thickness on the residual stress development during shot peening. High Performance Computing

in Science and Engineering'08, 481–492 (2009)
16 George, P. M., Pillai, N., Shah, N.: Optimization of shot peening parameters using Taguchi technique. Journal of Materials Processing Technology **153–154**, 925–930 (2004)
17 Guagliano, M., Vergani, L., Bandini, M., et al.: An approach to relate the shot peening parameters to the induced residual stresses. In: N. A ed. Proceedings of the 7th International Conference on Shot Peening, Warsaw, (1999)
18 Hirai, N., Tosha, K., Rouhaud, E.: Finite element analysis of shot peening on the form of a single dent. In: Proceedings of the 9th International Conference on Shot Peening, Paris, (2005)
19 Schwarzer, J., Schulze, V., Vohringer, O.: Finite element simulation of shot peening—a method to evaluate the influence of peening parameters on surface characteristics. In: Proceedings of the 8th International Conference on Shot Peening, Garmisch-Partenkirchen, Germany, (2002)
20 Hong, T., Ooi, J. Y., Shaw, B.: A numerical simulation to relate the shot peening parameters to the induced residual stresses. Engineering Failure Analysis **15**, 1097–1110 (2008)
21 Hong, T., Ooi, J. Y., Shaw, B. A.: A numerical study of the residual stress pattern from single shot impacting on a metallic component. Advances in Engineering Software **39**, 743–756 (2008)
22 Wu, X., Huang, C., Wang, X., et al.: A new effective method to estimate the effect of laser shock peening. International Journal of Impact Engineering **5**, 322–329 (2011)
23 Tan, Q. M.: Dimensional Analysis, (1st edn.) Chin. Univ. Sci. Technol. Press, Beijing (2005)
24 Buckingham, E.: On physically similar systems; illustrations of the use of dimensional equations. Physical Review **4**, 345–376 (1914)
25 Shivpuri, R., Cheng, X., Mao, Y.: Elasto-plastic pseudo-dynamic numerical model for the design of shot peening process parameters. Materials & Design **30**, 3112–3120 (2009)